Vol. 44 — N° 1 03 20 p. 69 – 83

GEOSTANDARDS and GEOANALYTICAL RESEARCH

NanoSr – A New Carbonate Microanalytical Reference Material for *In Situ* Strontium Isotope Analysis

Michael **Weber** (1, 2)*, Federico **Lugli** (3, 4), Bodo **Hattendorf** (5), Denis **Scholz** (1), Regina **Mertz-Kraus** (1), Damien **Guinoiseau** (2, 6) and Klaus Peter **Jochum** (2)

(1) Institute of Geosciences, Johannes Gutenberg University Mainz, J.-J.-Becher-Weg 21, 55128, Mainz, Germany
(2) Climate Geochemistry Department, Max Planck Institute for Chemistry, Hahn-Meitner-Weg 1, 55128, Mainz, Germany
(3) Department of Chemical and Geological Sciences, University of Modena and Reggio Emilia, Via Campi 103, 41125, Modena, Italy
(4) Department of Cultural Heritage, University of Bologna, 48121, Ravenna, Italy
(5) Laboratory of Inorganic Chemistry, ETH Zürich, Vladimir Prelog Weg 1,8093, Zürich, Switzerland
(6) Institut de Physique du Globe de Paris, Université de Paris, 1 Rue Jussieu, 75005, Paris, France
* Corresponding author. e-mail: michael.weber@uni-mainz.de

The *in situ* measurement of Sr isotopes in carbonates by MC-ICP-MS is limited by the availability of suitable microanalytical reference materials (RMs), which match the samples of interest. Whereas several well-characterised carbonate reference materials for Sr mass fractions > 1000 μg g^{-1} are available, there is a lack of well-characterised carbonate microanalytical RMs with lower Sr mass fractions. Here, we present a new synthetic carbonate nanopowder RM with a Sr mass fraction of *ca.* 500 μg g^{-1} suitable for microanalytical Sr isotope research ('NanoSr'). NanoSr was analysed by both solution-based and *in situ* techniques. Element mass fractions were determined using EPMA (Ca mass fraction), as well as laser ablation and solution ICP-MS in different laboratories. The $^{87}Sr/^{86}Sr$ ratio was determined by well-established bulk methods for Sr isotope measurements and is 0.70756 ± 0.00003 (2*s*). The Sr isotope microhomogeneity of the material was determined by LA-MC-ICP-MS, which resulted in $^{87}Sr/^{86}Sr$ ratios of 0.70753 ± 0.00007 (2*s*) and 0.70757 ± 0.00006 (2*s*), respectively, in agreement with the solution data within uncertainties. Thus, this new reference material is well suited to monitor and correct microanalytical Sr isotope measurements of low-Sr, low-REE carbonate samples. NanoSr is available from the corresponding author.

Keywords: strontium isotopes, laser ablation, reference material, calcium carbonate, nanopowder, MC-ICP-MS.

Received 23 May 19 – Accepted 10 Sep 19

The analysis of geological samples with state-of-the-art analytical techniques relies on the quality and availability of well-characterised reference materials (RMs). These RMs are a prerequisite for calibration, method validation, quality control and the establishment of metrological traceability (Jochum and Enzweiler 2014). In comparison with solution-based analytical techniques, *in situ* analyses, such as LA-(MC-)ICP-MS or SIMS, of unknown samples are limited by the availability of suitable RMs with microhomogeneity in the range of the respective test portion masses (μg–ng range). Furthermore, for laser ablation analysis, a similar matrix composition and mass fraction of the element of interest of the RM and the unknown sample are preferable (Jochum and Enzweiler 2014), in particular if femtosecond laser ablation systems are not available (Poitrasson *et al.* 2003, Vanhaecke *et al.* 2010).

Strontium isotopes are widely used by the geochemical community and applied in several different research fields, such as petrology, archaeology, palaeontology, palaeoclimatology, stratigraphy, forensics and food traceability (Kelly *et al.* 2005, Zhou *et al.* 2009, McArthur *et al.* 2012, Kimura *et al.* 2013, Durante *et al.* 2015, Lin *et al.* 2015, Bolea-Fernandez *et al.* 2016, Willmes *et al.* 2016, Lugli *et al.* 2017, 2018, Weber *et al.* 2018b). However, for the application of radiogenic Sr isotopes to carbonate samples, the availability of suitable microanalytical reference materials (MRMs) for *in situ* analyses is limited. Typical carbonate RMs with well-specified $^{87}Sr/^{86}Sr$ ratios, such as JCt-1, JCp-1 (both Geological Survey of Japan), FEBS-1 (National Research Council of Canada, NRCC) and MACS-3 (U.S. Geological Survey, USGS), have a high-Sr mass fraction > 1000 μg g^{-1} (Ohno and Hirata 2007, Yang *et al.* 2011,

doi: 10.1111/ggr.12296

Jochum *et al.* 2011b, Weber *et al.* 2018a) and are therefore mainly suited for *in situ* analyses of carbonate samples with similar mass fractions (e.g., corals, molluscs and otoliths). USGS MACS-1 is a low-Sr carbonate RM with known Sr isotope signature, but the high mass fraction of REEs (especially Dy, Er and Yb) limits its use as an *in situ* RM due to isobaric interferences of the doubly charged REEs (Weber *et al.* 2018a). Furthermore, not all available RMs show microanalytical homogeneity and potentially need further processing, that is, by milling protocols (Garbe-Schönberg and Müller 2014). In contrast to glass RMs with a broad availability and a large range of different compositions (Jochum *et al.* 2011a, b, Evans and Müller 2018), the number of available carbonate RMs below 1000 μg g^{-1} suitable for microanalytical Sr isotope analysis is limited. Especially for MC-ICP-MS systems with a narrow limitation of potential intensities on Faraday cups, RMs with similar mass fractions are necessary to use the same laser parameters for samples and RMs. This shows the need of carbonate microanalytical RMs with a relatively low-Sr mass fraction for *in situ* Sr isotope analysis of low-Sr, low-REE carbonates, such as speleothems. For this type of carbonates, the application of LA-MC-ICP-MS is currently restricted either to high-Sr samples (Weber *et al.* 2017, Wortham *et al.* 2017) or to solution-based analysis, which requires chemical separation prior to analysis (Banner *et al.* 1996, Goede *et al.* 1998, Zhou *et al.* 2009, Hori *et al.* 2013, Oster *et al.* 2014, Weber *et al.* 2018b).

Recent progress in the synthetic production of custom-made materials and further processing of established RMs enables the geochemical community to design very specific materials of different compositions and by different techniques (Tabersky *et al.* 2014, Garbe-Schönberg and Müller 2014, Bao *et al.* 2017, Wu *et al.* 2018, Jochum *et al.* 2019). One possibility is the flame spray technique, which allows production of materials with a nanoscale grain size and a customised composition and matrix for different applications. As has been shown for glass matrices (Tabersky *et al.* 2014), Avantama® (Stäfa, Switzerland) is capable of producing a synthetic material with a carbonate matrix and a specified mass fraction of the elements of interest. Therefore, Avantama® was able to produce a customised carbonate nanomaterial upon our request. The aim of this study was to characterise a material with a calcium carbonate matrix and a homogeneous mass fraction of Sr in the range of 500 μg g^{-1} ('NanoSr'), which can be used as matrix-matched reference material for LA-MC-ICP-MS studies of a variety of carbonate samples.

Material

Production of the carbonate nanopowder ('NanoSr') was performed in a similar way to that described by Tabersky *et al.* (2014). Details of the production are intellectual property of Avantama® and can therefore not be provided. The synthesis of the nanoparticles was performed by the flame spray technique using an organic precursor with the elements of interest incorporated (Athanassiou *et al.* 2010), resulting in a total amount of 15 g synthetic carbonate material with a specific mass fraction of Sr. Prior to all *in situ* measurements of the carbonate nanopowder, a hydraulic press (Perkin Elmer™, Waltham, MA, USA) was used to obtain a carbonate nanopowder pellet (~ 100 mg per pellet) with a diameter of 13 mm and a thickness of approximately 2 mm (Figure 1a) without using any additional binding material. The nanopowder was pressed for 15 min with a load of 5000 kg. The final nanopowder pellets were mechanically stable and glued to microscope slides for the *in situ* analyses. In total, nine different nanopowder pellets were produced and analysed.

Analytical techniques

To characterise the carbonate nanopowder, several analytical techniques were used. Electron probe microanalysis (EPMA) was used to determine the mass fraction of Ca. Trace element mass fractions were determined by ICP-MS and LA-ICP-MS in four different laboratories. The microhomogeneity of the carbonate nanopowder was tested using LA-ICP-MS at several different positions of the pressed nanopowder pellets, both in the inner and in the outer parts. Since the nanopowder was specifically designed for Sr isotope analyses, we determined the $^{87}Sr/^{86}Sr$ ratio by different techniques (TIMS and (LA-)MC-ICP-MS) in three different laboratories.

Element mass fractions

Element mass fractions were determined with three different types of instruments, by both solution-based (ICP-MS) and *in situ* techniques (EPMA and LA-ICP-MS) in five different laboratories.

Electron probe: For EPMA, a sample of the pressed nanopowder pellet was embedded in epoxy resin, polished, cleaned and covered with a ~ 20 nm layer of carbon by sputtering. Analysis was carried out at the Institute of Geosciences, Mainz, Germany, using a Jeol JXA 8200 microprobe in wavelength-dispersive spectrometry (WDS) mode. A beam current of 12 nA and an acceleration potential of 15 kV were used, with the electron beam defocused to 20 μm. Peak counting time was 20 s for Ca in double-channel mode. Raw data were corrected using the routine of Armstrong (1995), and a well-characterised carbonate reference material was used for calibration. In total, twenty-four measurements at different positions of the pressed nanopowder pellet were performed.

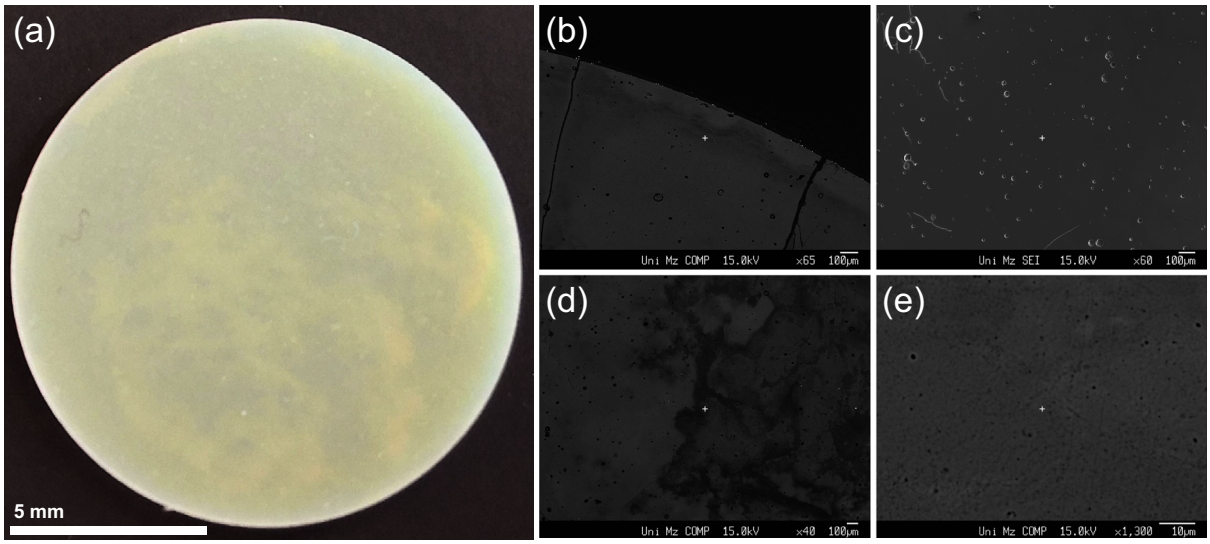

Figure 1. (a) Top view of a pressed nanopowder pellet with a diameter of 13 mm and a thickness of *ca.* 2 mm. (b) Backscattered electron (BSE) image of the edge of the compacted nanopowder pellet. (c) Top view of the compacted nanopowder pellet as secondary electron image (SEI). (d) Top view of the compacted nanopowder pellet showing darker and brighter areas in the BSE image. (e) BSE image of the compacted nanopowder pellet with a magnification of 1300, showing the compaction of the nanopowder and the small pore spaces below the µm range. [Colour figure can be viewed at wileyonlinelibrary.com]

Solution ICP-MS: Six aliquots of 5–10 mg of the carbonate nanopowder were dissolved in 3 mol l^{-1} HNO_3. Prior to the ICP-MS measurement, final acid concentration was adjusted to 0.8 mol l^{-1}. Elemental determinations of the digested nanopowder were performed using a quadrupole ICP-MS (Thermo Fisher Scientific, XSeries^{II}, Thermo Scientific, Bremen, Germany) housed at the Centro Interdipartimentale Grandi Strumenti (CIGS) of the University of Modena and Reggio Emilia. The samples were introduced into the mass spectrometer using a CETAC ASX 520 autosampler. The following signals were acquired during the session: ^{24}Mg, ^{85}Rb, ^{88}Sr, ^{138}Ba, ^{163}Dy, ^{166}Er and ^{172}Yb. A ^{115}In solution was aspirated and used as internal reference. A calibration was performed in the range 1–1000 ng g^{-1} using the IV-ICP-MS-71A multi-element standard solution (Inorganic Ventures), whereas the less abundant elements (e.g., Er, Dy, Er and Yb) were calibrated up to 200 ng g^{-1}.

LA-ICP-MS: Measurements by LA-ICP-MS were performed in three different laboratories. For all measurements, we employed ^{43}Ca as internal reference and used ^{85}Rb and ^{88}Sr for the calculation of trace element mass fractions. Initial data acquisition (approximately 3 s) of each measurement was discarded to prevent surface contamination potentially influencing our results.

Measurements at the Max Planck Institute for Chemistry (MPIC), Mainz, Germany, were performed using a New Wave UP213 Nd:YAG laser ablation system, coupled to a Thermo Finnigan Element 2 SF-ICP-MS. Spot analyses were performed at a repetition rate of 10 Hz, using a spot size of 80 µm with an energy output of 60%, resulting in a fluence of ~ 7.5 J cm^{-2}. Ablation time was set to 70 s. Line scan analyses were performed using a line length of 300 µm, a circular spot size of 55 µm, a repetition rate of 10 Hz, a transition speed of 5 µm s^{-1} and an energy output of 60%, resulting in a fluence of ~ 5 J cm^{-2}. Background signals for spot and line scan analyses were measured for 14 s, followed by the ablation and a washout time of 20 s. The following signals were monitored during the sessions: ^{25}Mg, ^{43}Ca, ^{85}Rb, ^{88}Sr, ^{137}Ba, ^{163}Dy, ^{167}Er and ^{173}Yb. For calibration purposes, NIST SRM 612 was analysed at the beginning, between each set of samples (n = 36) and at the end of the routine (n = 9). We used NIST SRM 610, USGS GSD-1G, GSE-1G and MACS-3 (each n = 9) as quality control materials (QCMs) to monitor accuracy and reproducibility (Table S1).

The trace element distribution within the nanopowder pellet was mapped by LA-ICP-MS at MPIC using MapIT! (Sforna and Lugli 2017). The LA-ICP-MS set-up was identical as described above, using NIST SRM 612 for calibration purposes and applying a total number of 66 line scans with a length of 13000 µm each, covering one half of the pressed nanopowder pellet (pellet 9). The spot size was set to 100 µm, using a transition rate of 30 µm s^{-1} and a repetition rate of 10 Hz with an energy output of 70%,

Table 1.
Operational parameters for the different (LA-MC-)ICP-MS systems used during this study

	ICP parameter	Value	Laser parameter [a]		Value	ICP parameter	Value	Laser parameter [a]		Value
Sr isotopes	*MC-ICP-MS Neptune*		*New Wave UP 213*			*MC-ICP-MS NU Plasma*		*New Wave UP 213*		
	Cool gas flow rate	15 l min^{-1}	*Ablation*	Spot size	100 μm	Cool gas flow rate	13 l min^{-1}	*Ablation*	Spot size	100 μm
	Auxiliary gas flow	0.8 l min^{-1}		Repetition rate	10 Hz	Auxiliary gas flow	0.93 l min^{-1}		Repetition rate	10 Hz
	Sample gas flow	0.9–1 l min^{-1}		Fluence	6 J cm^{-2}	Sample gas flow	0.75 l min^{-1}		Fluence	20–25 J cm^{-2}
	Plasma power	1200 W		Sampling scheme	Line	Plasma power	1300 W		Sampling scheme	Line
	Resolution	Low		Translation rate	5 μm s^{-1}	Resolution	Low		Translation rate	5 μm s^{-1}
	He flow rate [a]	0.6 l min^{-1}				He flow rate [a]	0.75 l min^{-1}			
Trace elements	*ICP-MS Element 2*		*New Wave UP 213*			*ICP-MS Agilent 7500ce*		*ESI NWR193*		
	Cool gas flow rate	16 l min^{-1}	*Ablation*	Spot size	55/80/100 μm	Cool gas flow rate	15 l min^{-1}	*Ablation*	Spot size	80 μm
	Auxiliary gas flow	1 l min^{-1}		Repetition rate	10 Hz	Auxiliary gas flow	0.9 l min^{-1}		Repetition rate	10 Hz
	Sample gas flow	0.6 l min^{-1}		Fluence	5–12.5 J cm^{-2}	Sample gas flow	0.8 l min^{-1}		Fluence	3.5 J cm^{-2}
	Plasma power	1150 W		Sampling scheme	Spot/Line	Plasma power	1200 W		Sampling scheme	Spot
	Resolution	Low		Dwell time	70 s	Resolution	0.65–0.75 [b]		Dwell time	60 s
	He flow rate [a]	0.75 l min^{-1}		Translation speed	5/30 μm s^{-1}	He flow rate [a]	0.8 l min^{-1}			
	ICP-MS XSeries^{II}		*New Wave UP 213*							
	Cool gas flow rate	13 l min^{-1}	*Ablation*	Spot size	100 μm					
	Auxiliary gas flow	1.08 l min^{-1}		Repetition rate	10 Hz					
	Sample gas flow	0.75 l min^{-1}		Fluence	5 J cm^{-2}					
	Plasma power	1400 W		Sampling scheme	Spot					
	Resolution	Low		Dwell time	60 s					
	He flow rate [a]	0.6 l min^{-1}								

[a] Only for laser ablation measurements. [b] (amu), peak width at 10% of its height.

resulting in a fluence of 12.5 J cm^{-2}. The following signals were monitored during the sessions: ^{25}Mg, ^{43}Ca, ^{85}Rb, ^{88}Sr and ^{137}Ba. For the imaging via MapIT!, no pre-ablation was performed.

Measurements by LA-ICP-MS at the Institute of Geosciences, were performed using an ArF Excimer 193 nm laser system (ESI NWR193) equipped with a TwoVol^2 ablation cell, coupled to an Agilent 7500ce ICP-MS. A spot size of 80 μm, a repetition rate of 10 Hz and a fluence of 3.5 J cm^{-2} were used. Fifteen seconds laser warm-up time was followed by 60 s of dwell time and 20 s of washout time. NIST SRM 612 was used for calibration purposes and measured at the beginning, between the set of samples (n = 36) and at the end of the routine (n = 9). For quality control, we used NIST SRM 610, USGS GSD-1G, GSE-1G, MACS-3 and BCR-2G (Table S2). The following signals were monitored during the sessions: ^{25}Mg, ^{43}Ca, ^{85}Rb, ^{88}Sr, ^{137}Ba, ^{163}Dy, ^{167}Er and ^{173}Yb. For all laser ablation measurements performed at MPIC and at the Institute of Geosciences, mass fractions for the RMs were obtained from GeoReM (Jochum *et al.* 2005), and data reduction was performed offline, following the calculations given in Mischel *et al.* (2017).

LA-ICP-MS analyses at the CIGS were performed using a 213 nm laser ablation system (New Wave UP) and a quadrupole ICP-MS (Thermo Scientific XSeries^{II}). The pressed nanopowder pellet (pellet 7) was analysed employing a spot size of 80 μm, a pulse repetition rate of 10 Hz and a fluence of ~ 5 J cm^{-2}. The surface of the nanopowder pellet was pre-ablated before each spot analysis. The following

signals were measured during the session: ^{43}Ca, ^{85}Rb, ^{88}Sr, ^{163}Dy and ^{172}Yb. NIST SRM 612 and GSJ JCt-1 were used as calibration materials. Data reduction was performed offline, following the calculations given in Mischel *et al.* (2017). Operating parameters for all LA-ICP-MS measurements are presented in Table 1.

Strontium isotopes

Radiogenic Sr isotope ratios were determined in five different laboratories, using both solution-based (TIMS and MC-ICP-MS) and *in situ* techniques (LA-MC-ICP-MS).

TIMS: Strontium separation was performed using Eichrom Sr-Spec™ ion exchange resin columns at CIGS as described for MC-ICP-MS in the next section. The Sr isotope composition of the carbonate nanopowder was determined by thermal ionisation mass spectrometry (TIMS) at the MPIC, Mainz, using a Thermo Scientific Triton. For that purpose, about 100 ng Sr was transferred onto a W filament, surrounded by a TaF activator. Measurements were performed in static multi-collection mode, simultaneously collecting *m/z* ratios representing ^{84}Sr, ^{85}Rb, ^{86}Sr, ^{87}Sr and ^{88}Sr for ten blocks of twenty cycles each (integration time of 16.8 s per cycle). All isotope ratios were corrected for internal mass fractionation using the stable ^{88}Sr/^{86}Sr ratio of 8.375209 (Berglund and Wieser 2011). The isobaric interference of ^{87}Rb on ^{87}Sr was corrected recording the ^{85}Rb peak and by using a ^{87}Rb/^{85}Rb of 0.386010. The intermediate measurement precision of the ^{87}Sr/^{86}Sr value for NIST SRM 987 was 0.710256 ± 0.000012 (2*s*, *n* = 25), in agreement with reported values in literature (McArthur *et al.* 2001).

MC-ICP-MS: Multi-collector ICP-MS measurements were performed at the CIGS and the MPIC. All samples were processed at the Laboratory of Isotope Geochemistry of the Department of Chemical and Geological Sciences (University of Modena and Reggio Emilia, Modena, Italy), following the protocol of Lugli *et al.* (2017) and Weber *et al.* (2018a). Around 5–10 mg of nanopowder was digested with 3 ml of 3 mol l^{-1} HNO_3 (suprapur) and loaded into 300 µl columns filled with Eichrom Sr-Spec™ resin (100–150 µm bead size). Matrix ions were removed by stepwise addition of 3 mol l^{-1} HNO_3. Strontium was then eluted with Milli-Q® water and collected in clean beakers. The final solutions were adjusted to 0.8 mol l^{-1} HNO_3. The entire procedure was conducted in a cleanroom equipped with a class 10 laminar flow hood.

To determine the ^{87}Sr/^{86}Sr ratio, a Neptune MC-ICP-MS was used at CIGS following Lugli *et al.* (2017). The following signals were collected simultaneously on seven Faraday cups equipped with 10^{11} Ω resistors: ^{82}Kr, ^{83}Kr, ^{84}Sr, ^{85}Rb, ^{86}Sr, ^{87}Sr and ^{88}Sr. Strontium solutions were diluted to ~ 250 ng g^{-1} and introduced into the mass spectrometer system through a quartz spray chamber using a 100 µl min^{-1} nebuliser. A static multi-collection mode with a single block of 100 cycles (integration time 8.4 s per cycle) was used to analyse the samples, as well as NIST SRM 987 and blanks. A bracketing sequence was employed to correct for instrumental drifts. Krypton as a potential contamination in the Ar gas was monitored and corrected using a ^{86}Kr/^{83}Kr ratio of 1.505657 (Berglund and Wieser 2011). To correct for the presence of isobaric Rb on *m/z* 87, a ^{87}Rb/^{85}Rb ratio of 0.3856656 (Berglund and Wieser 2011) was used. Mass bias normalisation was performed applying the exponential law, using the accepted ^{88}Sr/^{86}Sr ratio of 8.375209 (Steiger and Jäger 1977). We are aware of the observed natural variations in δ^{88}Sr (Fietzke and Eisenhauer 2006, Krabbenhöft *et al.* 2009); however, by convention, radiogenic Sr isotope measurements are usually corrected assuming the stable ^{88}Sr/^{86}Sr ratio (Fietzke *et al.* 2008), which we follow within this study. In addition, variability in ^{87}Sr/^{86}Sr is far greater than the whole range reported for stable Sr isotopes ratios in literature. Rubidium mass bias was assumed to be the same as for Sr. Daily repeated measurements of NIST SRM 987 yielded a mean ^{87}Sr/^{86}Sr ratio of 0.71024 ± 0.00001 (2*s*; *n* = 20). Strontium isotope ratios of the samples were corrected to the NIST SRM 987 ^{87}Sr/^{86}Sr ratio of 0.710248 (McArthur *et al.* 2001).

Sr isotope ratios at the MPIC were determined using a Nu Plasma MC-ICP-MS coupled to a CETAC Aridus II desolvating nebuliser system, following the methods described by Lugli *et al.* (2017). Samples were diluted to ~ 100 ng g^{-1}, and the following signals were monitored using Faraday cups equipped with 10^{11} Ω resistors during analysis: ^{82}Kr, ^{83}Kr, ^{84}Sr, ^{85}Rb, ^{86}Sr, ^{87}Sr and ^{88}Sr. Analysis was performed in a calibrator-bracketing sequence, using a static multi-collection mode with 100 cycles and an integration time of 5 s. Krypton and Rb correction was performed as described for the measurements at CIGS. Repeated measurements of NIST SRM 987 yielded a mean ^{87}Sr/^{86}Sr ratio of 0.71030 ± 0.00003 (2*s*; *n* = 10). Resulting ^{87}Sr/^{86}Sr ratios were corrected to the NIST SRM 987 ^{87}Sr/^{86}Sr ratio of 0.710248 (McArthur *et al.* 2001).

LA-MC-ICP-MS: Microanalytical homogeneity for Sr isotopes was investigated using LA-MC-ICP-MS at the MPIC and the CIGS. Operational parameters for both (LA-)MC-ICP-MS systems are provided in Table 1. Analyses at the MPIC were performed following the protocol of Weber *et al.* (2017) using a Nu Plasma MC-ICP-MS coupled to a New Wave UP213 Nd:YAG laser ablation system. Peak shape

and coincidence for the Sr isotopes of interest (^{84}Sr, ^{86}Sr, ^{87}Sr, ^{88}Sr) were tuned using the Sr reference solution NIST SRM 987, while the mass spectrometer was coupled to a CETAC Aridus II desolvating nebuliser system, prior to connecting the laser ablation system. For the laser ablation measurements, line scans of 750 μm length with a spot size of 100 μm, a translation speed of 5 μm s^{-1} and an energy output of 80% were applied, resulting in a fluence of 20–25 J cm^{-2}. Pre-ablation was performed prior to each analysis. Krypton was corrected by subtracting the on-peak baseline during the laser warm-up time (45 s). Interferences of REEs were corrected by monitoring ^{171}Yb and ^{167}Er. Molecular interferences were found to be negligible by monitoring *m/z* 82 and 83 (signals usually below 0.2 mV, see Vroon *et al.* (2008), Woodhead *et al.* (2005)). Mass bias correction was performed using the exponential law (Ingle *et al.* 2003) and an $^{88}Sr/^{86}Sr$ ratio of 8.375209 (Steiger and Jäger 1977). Mass/charge 85 was used to monitor the occurrence of ^{85}Rb and to correct *m/z* 87 by calculating the fraction of ^{87}Rb using the constant $^{87}Rb/^{85}Rb$ ratio of 0.3857 (Berglund and Wieser 2011).

Analyses at the CIGS were performed using a Neptune MC-ICP-MS coupled to a New Wave UP213 Nd:YAG laser ablation system, following the method described by Lugli *et al.* (2017). Nine Faraday detectors equipped with 10^{11} Ω resistors were employed to acquire peaks of ^{82}Kr, ^{83}Kr, ^{84}Sr, ^{85}Rb, ^{86}Sr, ^{87}Sr and ^{88}Sr as well as the doubly charged $^{171}Yb^{2+}$ and $^{173}Yb^{2+}$. For the LA measurements, we employed a linear raster of 100 × 500 μm, a fluence of ~ 6 J cm^{-2}, a repetition rate of 10 Hz and a scan speed of 5 μm s^{-1}. Prior to each analysis, the sample was pre-ablated to avoid surface contaminations. A He flow of *ca.* 0.6 l min^{-1} was used to carry the ablated material into the mass spectrometer. Krypton was corrected by subtracting the on-peak baseline during the laser warm-up (~ 60 s). Rare-earth element and Ca dimers/argides were monitored, but not corrected because their interference with the analyses is negligible. Mass bias and Rb were corrected as previously reported for the measurements performed at the MPIC. During the measurement session, we also measured a modern marine bivalve shell as an in-house reference material, which yielded an $^{87}Sr/^{86}Sr$ ratio of 0.70916 ± 0.00002 (2SE, *n* = 1), in agreement with the modern seawater value (McArthur *et al.* 2012).

Results

Calcium mass fractions

EPMA yielded a CaO value of 52.6 ± 1.5% *m/m* (*n* = 24, 2*s*, pellet 8), equivalent to a Ca mass fraction of 376000 ± 11000 μg g^{-1} (*n* = 24, 2*s*, pellet 8, Table S13). These measurements were performed at different positions of the pressed nanopowder pellet, in both the brighter and darker areas (Figure 1d) and did not yield significantly different results. The overall uncertainty of the Ca mass fraction obtained by EPMA was about 3% and therefore in a similar range as expected for the (LA-)ICP-MS analyses. Therefore, we used the resulting Ca mass fraction of 376000 ± 11000 μg g^{-1} (*n* = 24, 2*s*) as the internal reference for the calibration of the trace element determinations.

Mass fractions of Sr and potential interfering elements

Solution-based ICP-MS yielded a mean Sr mass fraction of 495 ± 51 μg g^{-1} (*n* = 6, 2*s*) for NanoSr. Analyses of potential interfering materials resulted in mean mass fractions < 0.2 μg g^{-1} (Figure 2). Rubidium, as a major potential isobaric interference for *in situ* Sr isotope analyses, yielded a mean mass fraction of 0.075 ± 0.036 μg g^{-1} (*n* = 6, 2*s*). This results in a maximum Rb/Sr ratio of 0.0002, much lower than the suggested Rb/Sr threshold of 0.02 for successful LA-(MC-)ICP-MS measurements of Sr isotopes (Irrgeher *et al.* 2016). Further potential interfering elements yielded very low mass fractions (Dy = 0.16 ± 0.04 μg g^{-1}; Er = 0.02 ± 0.04 μg g^{-1}; Yb = 0.05 ± 0.04 μg g^{-1}, all uncertainties (2*s*) are for *n* = 6) and are thus considered to be negligible for *in situ* Sr isotope measurements, as has been shown for reference materials with a higher mass fraction of these elements (Weber *et al.* 2018a).

Mass fractions of Sr and Rb were determined by LA-ICP-MS in three different laboratories as described above. The results are shown in Figure 3. Analyses from the Institute of Geosciences (Figure 3a), yielded a mean mass fraction of 483.7 ± 11.5 μg g^{-1} for Sr and of 0.05 ± 0.02 μg g^{-1} for Rb (*n* = 72, 2*s*, pellets 1–6, for both Sr and Rb). Results from CIGS (Figure 3b) show mean mass fractions of 501.7 ± 8.3 μg g^{-1} for Sr and 0.05 ± 0.02 μg g^{-1} for Rb (both *n* = 5, 2*s*, pellet 7) and are in good agreement with the results from the Institute of Geosciences. Analyses at MPIC were performed by spot (Figure 3c) and line scan analyses (Figure 3d). Spot analyses yielded a mean mass fraction of 505.4 ± 11.5 μg g^{-1} for Sr and 0.071 ± 0.005 μg g^{-1} for Rb (both *n* = 72, 2*s*, pellets 1–6), while line scan analyses resulted in a mean mass fraction of 479.1 ± 26.2 μg g^{-1} for Sr and 0.062 ± 0.009 μg g^{-1} for Rb (both *n* = 18, 2*s*). An overview of the mass fractions of the elements of interest determined by the different analytical techniques is provided in Table 2. Barium (< 0.20 ± 0.03 μg g^{-1}) mass fraction is provided to indicate the purity of the carbonate

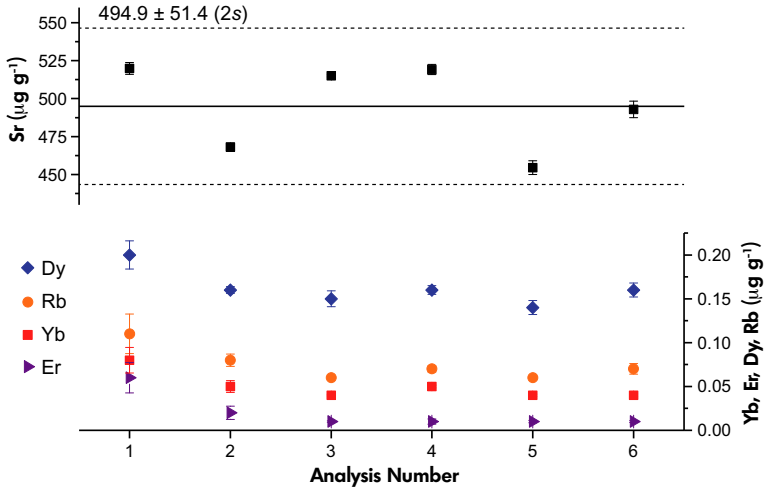

Figure 2. Solution-based ICP-MS results for the mass fractions of Sr (black square, top graph) and Yb (red square), Er (purple triangle), Dy (blue diamond) and Rb (orange circle, bottom graph) for digestion of six samples. The horizontal black line represents the mean mass fraction of Sr (495 ± 51 µg g^{-1}, *n* = 6) with the respective 2*s* uncertainties expressed as dashed lines. All uncertainties in the bottom panel are 2*s*. [Colour figure can be viewed at wileyonlinelibrary.com]

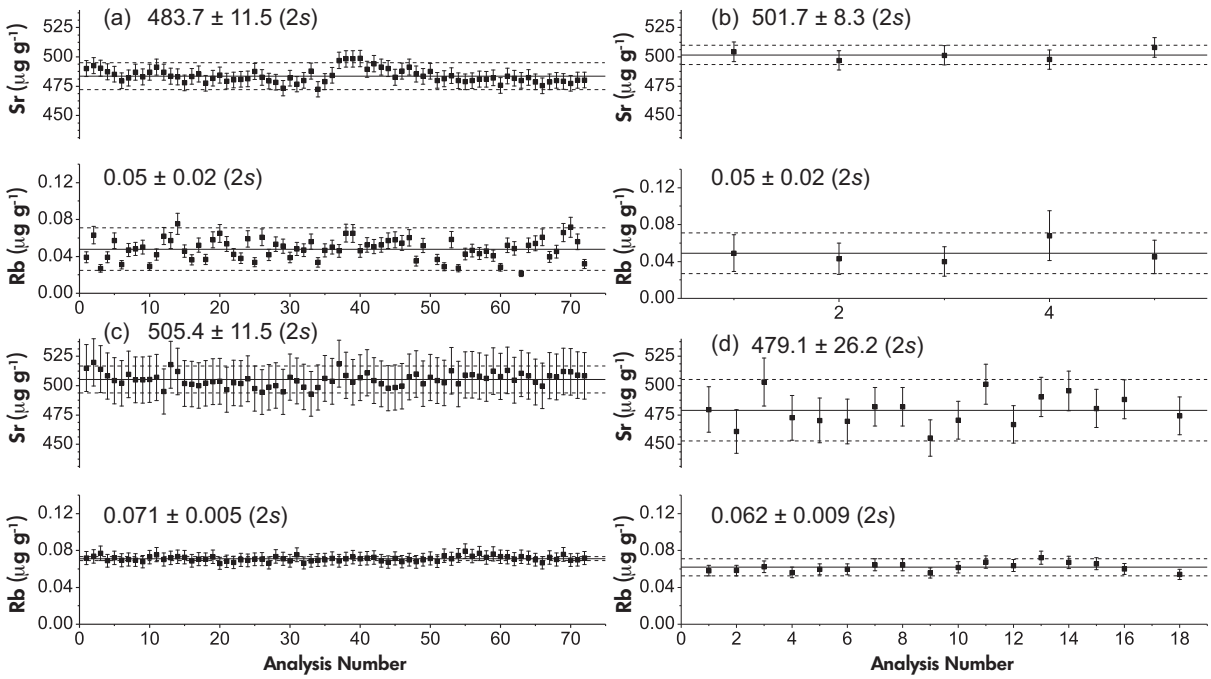

Figure 3. LA-ICP-MS results obtained in different laboratories. In total, seven different nanopowder pellets were analysed. (a) Strontium and Rb mass fractions obtained at the Institute of Geosciences, Mainz (*n* = 72, pellets 1–6). (b) Strontium and Rb mass fractions obtained at the CIGS, Modena (*n* = 5, pellet 7). (c) Strontium and Rb mass fractions obtained at MPIC, Mainz, by spot (*n* = 72, pellets 1–6) and (d) line scan analyses (*n* = 18, pellet 1). The horizontal black line represents the mean mass fractions for Sr and Rb with the respective 2*s* uncertainties expressed as dashed lines. All uncertainties of single measurements are 1*s*.

material. All laser ablation analyses performed in this study are in agreement with the results obtained by solution ICP-MS within uncertainty.

Further determinations of major element mass fractions by EPMA did not show large contributions (see Table S14). Results of BaO, MgO, K_2O and MnO were below the detection limit, while FeO and Na_2O yielded mean values of 0.015 ± 0.016 and 0.020 ± 0.032% *m/m* (*n* = 9, 2*s*), respectively.

Trace element imaging

The results from the imaging using MapIT! are presented in Figure 4. The mass fraction of Sr is between 450 and 500 μg g^{-1}, does not show any significant variability and is thus homogeneously distributed across the pressed nanopowder pellet (pellet 9). Individual pixels however resulted in substantially higher values, which might be related to a heterogeneous distribution but is considered more likely to be caused by instrumental artefacts. Rubidium as a major potential interference for *in situ* analyses of Sr isotopes only has a very low mass fraction (< 0.2 μg g^{-1}), although yielding higher values than obtained by the other methods (Table 2 and Figure 3). However, the Rb mass fraction is still sufficiently low to not affect the Sr isotope measurements significantly (Irrgeher *et al.* 2016). Magnesium and Ba are usually minor components of carbonate materials and were therefore monitored for the NanoSr pellet. Barium does not show substantial variability and is generally below 0.2 μg g^{-1}. Magnesium, in contrast, exhibits areas of higher mass fraction, especially at the edge of the nanopowder pellet, which were caused by spikes in the data and are therefore considered to be an artefact. No pre-ablation was performed prior to the mapping, so either Mg contained in the glue, molecular ions (e.g., C_2 with m/z = 24) from organic components in the glue, or Mg contamination during the production/postproduction processes. In general, the Mg mass fraction is low (< 5 μg g^{-1}) and is unlikely to affect Sr isotope analysis, even if Mg is not entirely homogeneous within the nanopowder pellet. All imaged element mass fractions are in reasonable agreement with the conventional element mass fractions obtained by (LA-) ICP-MS, although showing some general noise in the element distribution, which is usually common for mapping techniques (Sforna and Lugli 2017).

Solution Sr isotope measurements

The $^{87}Sr/^{86}Sr$ ratio determined by TIMS yielded a mean ratio of 0.707563 ± 0.000009 (2*s*, *n* = 6), which is in agreement with both MC-ICP-MS analyses (Table 3). The $^{84}Sr/^{86}Sr$ ratio obtained by TIMS yielded a mean ratio of 0.056493 ± 0.000003 (2*s*, *n* = 6). Strontium isotope determinations at CIGS yielded a mean $^{87}Sr/^{86}Sr$ ratio of 0.70755 ± 0.00001 (2*s*, *n* = 19) and a mean $^{84}Sr/^{86}Sr$ ratio of 0.05648 ± 0.00001 (2*s*, *n* = 19, Figure 5a). A pressed nanopowder pellet was dissolved to monitor potential contamination during the nanopowder pellet production. The results for this nanopowder pellet agree with the other samples, both for $^{87}Sr/^{86}Sr$ (0.70755 ± 0.00001, 2SE) and for $^{84}Sr/^{86}Sr$ (0.056488 ± 0.000002, 2SE, Figure 5a white square). Strontium isotope ratios determined at the MPIC agree within uncertainty with the data obtained at CIGS. The mean $^{87}Sr/^{86}Sr$ ratio is 0.70756 ± 0.00004 (2*s*, *n* = 21), and the mean $^{84}Sr/^{86}Sr$ ratio is 0.05648 ± 0.00010 (2*s*, *n* = 21, Figure 5b). Again, the analysis of the previously pressed sample did not significantly deviate from the other measurements for $^{87}Sr/^{86}Sr$ (0.70758 ± 0.00002, 2SE) and $^{84}Sr/^{86}Sr$ (0.056535 ± 0.000010, 2SE, Figure 5b white square). Analyses performed with the Neptune MC-ICP-MS show a better reproducibility than those obtained with the Nu MC-ICP-MS at MPIC for both $^{87}Sr/^{86}Sr$ and $^{84}Sr/^{86}Sr$. This is most likely related to the higher sensitivity of the Neptune system and does not represent inhomogeneity of the NanoSr powder. In summary, all solution-based techniques yielded the same results for the $^{87}Sr/^{86}Sr$ ratio of the NanoSr with a mean ratio of 0.70756 ± 0.00003 (2*s*, *n* = 46).

Laser ablation Sr isotope measurements

Laser ablation Sr isotope measurements were performed at two different laboratories to validate the microhomogeneity of the carbonate nanopowder in terms of Sr isotope signature. The $^{87}Sr/^{86}Sr$ ratios as well as the $^{84}Sr/^{86}Sr$ ratios showed a greater variability in comparison with the solution data. However, the $^{87}Sr/^{86}Sr$ ratio agrees within uncertainty with the solution data with a mean ratio of 0.70753 ± 0.00007 (2*s*, *n* = 58, Figure 6a, pellets 1–6) for the analyses at the MPIC, and a mean ratio 0.70757 ± 0.00006 (2*s*, *n* = 10, Figure 6b, pellet 7) for the analyses at the CIGS. The mean $^{84}Sr/^{86}Sr$ at MPIC was 0.05617 ± 0.00024 (2*s*, *n* = 58, Figure 6a, pellets 1–6). The $^{84}Sr/^{86}Sr$ ratios obtained at CIGS were significantly higher and agree with the natural ratio with a mean ratio of 0.05656 ± 0.00012 (2*s*, *n* = 10, Figure 6b, pellet 7). Again, the analyses performed with the Neptune system show a better reproducibility than those performed with the Nu MC-ICP-MS system. To allow traceability of the obtained data set, three international microanalytical carbonate RMs (JCt-1, JCp-1 and MACS-3) were analysed at MPIC using the same instrumentation and methodology. All $^{87}Sr/^{86}Sr$ ratios of the analysed RMs are within the expected literature values (see Weber *et al.* (2018a) and references therein), yielding Sr isotope ratios of $^{87}Sr/^{86}Sr$ = 0.70918 ± 0.00008

Table 2.
Mass fractions of Mg, Rb, Sr, Ba, Dy, Er and Yb, as well as respective test portion mass for the different analytical techniques

	Mg (μg g^{-1})	Rb (μg g^{-1})	Sr (μg g^{-1})	Ba (μg g^{-1})	Dy (μg g^{-1})	Er (μg g^{-1})	Yb (μg g^{-1})	Test portion mass (μg)
LA-ICP-MS[1]Spot analysis	2.7 ± 0.4	0.05 ± 0.02	483.7 ± 11.5	b.d.l.	0.13 ± 0.03	b.d.l.	b.d.l.	0.8–1.0
LA-ICP-MS[2]Spot analysis	NA	0.05 ± 0.02	501.7 ± 8.3	0.17 ± 0.06	0.20 ± 0.02	NA	0.05 ± 0.02	1.5–2.0
ICP-MS[2]Bulk	NA	0.08 ± 0.02	494.9 ± 51.4	0.21 ± 0.05	0.16 ± 0.02	0.02 ± 0.02	0.05 ± 0.02	5000–10000
LA-ICP-MS[3]Spot analysis	3.1 ± 0.2	0.07 ± 0.01	505.4 ± 11.5	0.18 ± 0.04	0.18 ± 0.01	0.004 ± 0.002	0.04 ± 0.01	1.5–2.0
LA-ICP-MS[3]Line scan	3.0 ± 0.5	0.06 ± 0.01	479.1 ± 26.2	0.17 ± 0.04	0.20 ± 0.03	0.004 ± 0.010	0.05 ± 0.02	0.4–0.5

Typical RSF (relative sensitivity factor) values for carbonate reference materials used during data acquisition usually agree within 10% uncertainty with the GeoReM values (Jochum *et al.* 2005) for all presented elements (Tables S1 and S2).
Individual results for (LA-)ICP-MS measurements are provided in Tables S3–S7.
1 = Institute of Geosciences, Mainz; 2 = CIGS, Modena; 3 = MPIC, Mainz; NA = not available, b.d.l. = below detection limit.

and $^{84}Sr/^{86}Sr$ = 0.05635 ± 0.00006 for JCt-1 (2*s*, *n* = 10), $^{87}Sr/^{86}Sr$ = 0.70917 ± 0.00007 and $^{84}Sr/^{86}Sr$ = 0.05603 ± 0.00006 for JCp-1 (2*s*, *n* = 10) and $^{87}Sr/^{86}Sr$ = 0.70757 ± 0.00004 and $^{84}Sr/^{86}Sr$ = 0.05637 ± 0.00007 for MACS-3 (2*s*, *n* = 10).

Discussion

For any microanalytical RMs (MRMs), homogeneity is a fundamental requirement. This should be true for element and isotope composition in case the MRM is used for *in situ* isotope studies, independent on the typical test portion mass used for analysis (Kane *et al.* 2003). We therefore used techniques with different test portion masses, that is, solution-based vs. laser ablation, to test homogeneity on the ng–μg range and check whether potential inhomogeneity in this range can influence the resulting $^{87}Sr/^{86}Sr$ ratios obtained by LA-MC-ICP-MS.

Element mass fraction

The Ca mass fraction was determined by EPMA in both the darker and brighter areas of the compacted nanopowder pellet (Figure 1d) and yielded a mean value of 376000 ± 11000 μg g^{-1} (*n* = 24, 2*s*, pellet 8) and did not show significant differences. As shown in Figure 1e, the pore space of the pressed nanopowder pellet is < 1 μm, indicating a well-compacted material, which is a prerequisite for microhomogeneity. In addition, the Ca mass fraction is in good agreement with Ca mass fractions commonly used for LA-ICP-MS trace element determinations in carbonates, where Ca is used as an internal reference (e.g., Jochum *et al.* 2005, 2012, Mischel *et al.* 2017, Weber *et al.* 2018b), although it is slightly lower than expected from the stoichiometric value CaO for calcium carbonate of 56.03% *m/m*. For the use as a Sr isotope reference material, the precise knowledge of the Ca mass fraction is not relevant for calibration purposes. Besides Ca, only very small major element contributions have been observed for NanoSr, indicating a pure calcium carbonate matrix, similar to the intended samples for Sr isotope analysis, such as speleothems.

Solution analysis of the synthetic carbonate nanopowder revealed a mean Sr mass fraction of 495 ± 51 μg g^{-1} (2*s*). *In situ* analyses at different laboratories revealed Sr mass fraction of the nanopowder pellet ranging from 479 ± 26 to 505 ± 20 μg g^{-1}. However, all laser ablation results lie within the uncertainty range of each other and the solution measurements. Furthermore, the variability during 1 day of measurement and within one laboratory did not exceed the 2*s* uncertainty of the bulk analysis. The imaging of the nanopowder pellet also showed minor Sr variability in the 2*s* range of the conventional LA-ICP-MS analysis, implying that the material is suitable for microanalysis. The small differences between the different laboratories could be caused by the different ablation conditions, calibration strategies and instruments used for this study, as has been recently shown for several common glass and carbonate RMs (Evans and Müller 2018).

The mean Sr mass fraction of the new synthetic carbonate reference material is 495 ± 51 μg g^{-1}, which was the overall aim prior to production. Since the material is mainly intended for *in situ* Sr isotope studies, a variability of the element mass fraction in the range observed in this study is not expected to affect the intended use. Potential interfering elements, such as Rb and the REEs, were found not to be incorporated in the nanopowder at significant levels. The Rb mass fraction was found to be < 0.2 μg g^{-1} and the mathematical correction does thus not impose a substantial limitation for the application for *in situ* Sr isotope

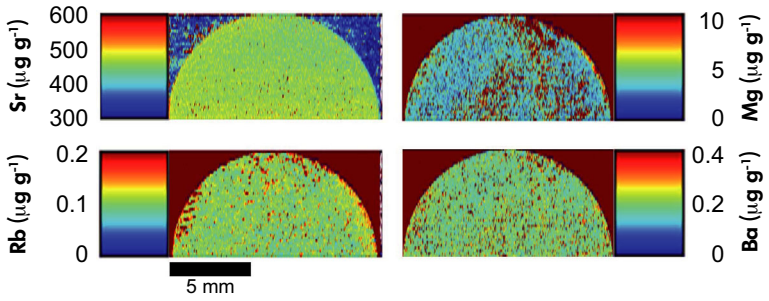

Figure 4. Element distribution for Sr (top left), Rb (bottom left), Mg (top right) and Ba (bottom right) of the pressed nanopowder pellet (pellet 9) obtained with the MapIT! software (Sforna and Lugli 2017). The upper half of the nanopowder pellet was analysed. The length of the *x*-axis is 13 mm (diameter of the pellet) and the y-distance 6.6 mm for each image obtained. [Colour figure can be viewed at wileyonlinelibrary.com]

Table 3.
$^{87}Sr/^{86}Sr$ and $^{84}Sr/^{86}Sr$ ratios for the different analytical techniques with the respective test portion masses of the measurements

	$^{87}Sr/^{86}Sr$	$^{84}Sr/^{86}Sr$	Test portion mass [a] (µg)	No. of analyses
TIMS[1]	0.70756 ± 0.00001	0.056493 ± 0.000003	2500–5000	6
MC-ICP-MS[1]	0.70756 ± 0.00004	0.05648 ± 0.00010	2500–5000	21
MC-ICP-MS[2]	0.70755 ± 0.00001	0.05648 ± 0.00001	2500–5000	19
LA-MC-ICP-MS[1]	0.70753 ± 0.00007	0.05617 ± 0.00024	2–3	58
LA-MC-ICP-MS[2]	0.70757 ± 0.00006	0.05656 ± 0.00012	2–3	10
NanoSr, 2*s*	0.70756 ± 0.00003			46
NanoSr, 95% CL	0.707558 ± 0.000009			46

The resulting $^{87}Sr/^{86}Sr$ ratio for NanoSr is the mean of all solution-based measurements. All uncertainties are given as 2*s*. The mean $^{87}Sr/^{86}Sr$ ratio based on a 95% confidence level (CL) is also provided. Indivdual results for Sr isotopes are provided in Tables S8–S12.
1 = MPIC, Mainz, 2 = CIGS, Modena; NA = not available.
[a] The test portion mass for the solution-based analyses takes the total amount of sample material into account, which was dissolved and homogenised for each aliquot. The actual Sr amount used for the measurements is usually much smaller, that is, 100 ng for TIMS and 50–500 ng for MC-ICP-MS, depending on the analysis time and used mass fraction for analysis.

studies. Imaging of the Rb distribution in the nanopowder pellet did not reveal areas of significantly higher mass fraction. REE mass fractions were determined by solution ICP-MS and are too low (< 0.2 µg g^{-1}) to influence the resulting $^{87}Sr/^{86}Sr$ ratios during LA-MC-ICP-MS. Therefore, doubly charged REEs, which would potentially hamper the quality of the results, are not expected to affect Sr isotope ratio measurements. Our data show that no significant contamination with any other relevant element occurred during material production or during the preparation of the nanopowder pellet.

Strontium isotope composition

The primary aim for producing the new NanoSr as MRM was to create a material for matrix-matched calibration of *in situ* Sr isotope analyses of carbonate samples with low-Sr abundance. Therefore, it is highly important to precisely characterise the Sr isotope signature of this material. In this study, the material was analysed in five different laboratories using TIMS, two different MC-ICP-MS and two different LA-MC-ICP-MS systems. All Sr isotope measurements yield identical results within uncertainty. We further analysed a sample, which was previously pressed as a nanopowder pellet and then dissolved for the solution analysis to investigate the potential contamination during pellet production. The results of these measurements agree with the overall mean Sr isotope ratio. Therefore, we define a Sr isotope ratio of 0.70756 ± 0.00003 (2*s*, *n* = 46) for NanoSr (Table 3).

Furthermore, the solution analyses yielded, within uncertainty, the same mean ratio as the LA-ICP-MS method, although the large test portion masses of the solution-based analyses are not considering potential inhomogeneities in the µg range, which is usually the test portion mass for *in situ*

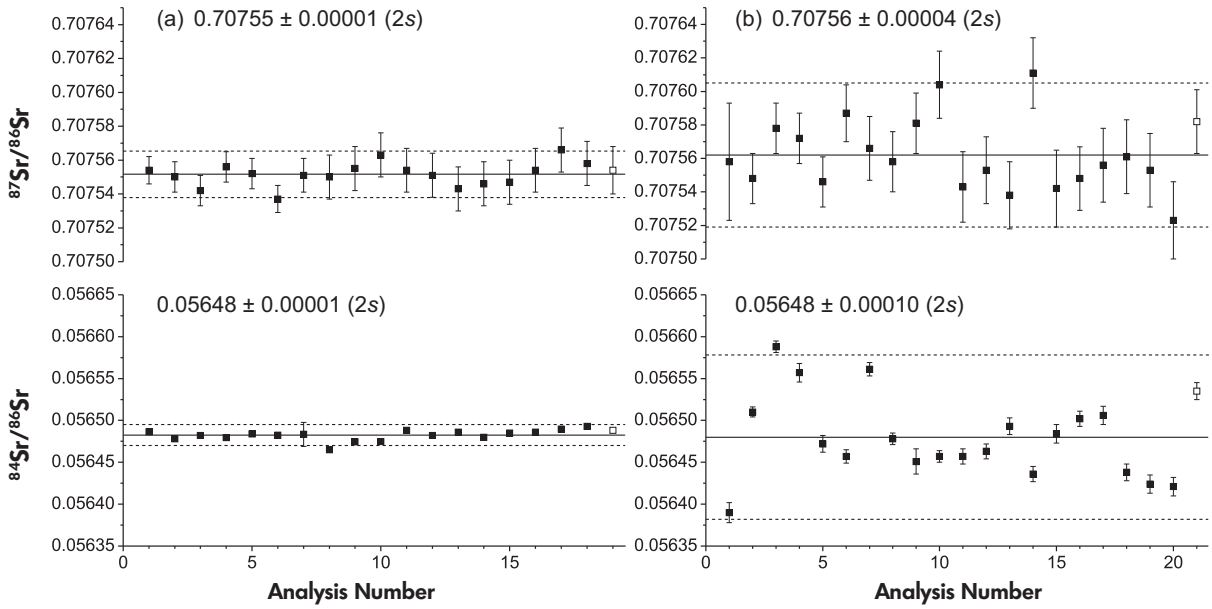

Figure 5. (a) MC-ICP-MS Neptune data from CIGS (*n* = 19). (b) MC-ICP-MS Nu Plasma data from MPIC (*n* = 21). Black squares represent the $^{87}Sr/^{86}Sr$ and $^{84}Sr/^{86}Sr$ ratios, respectively, of the individual measurements. Horizontal black lines show the mean ratios with the corresponding 2*s* uncertainties as dashed lines. White squares represent results from the pressed nanopowder pellet, which was dissolved for solution analysis.

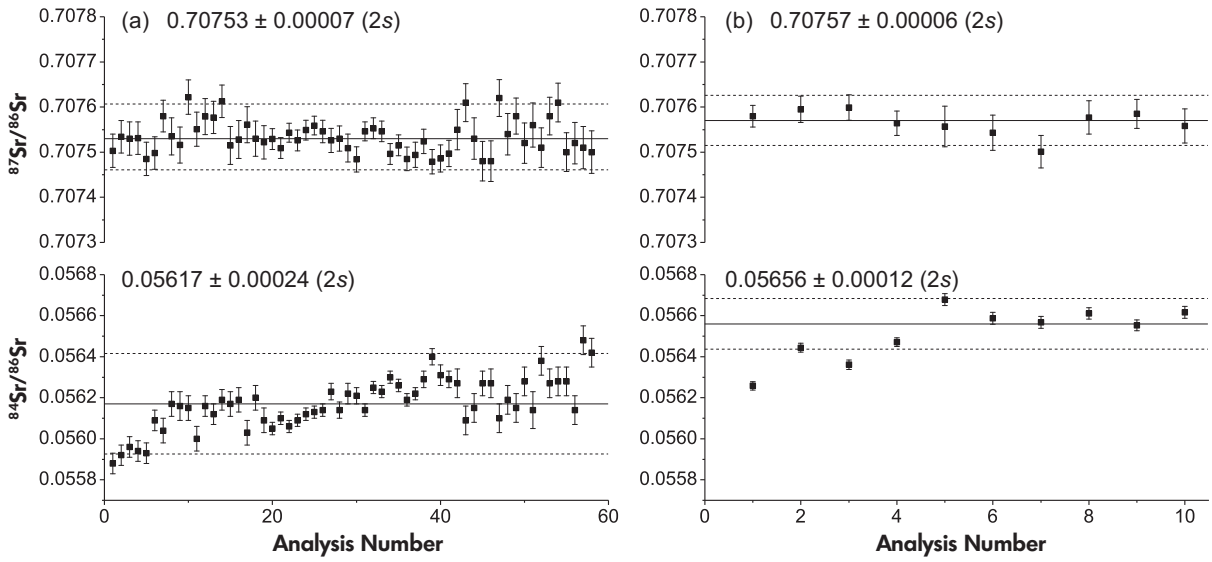

Figure 6. Laser ablation MC-ICP-MS data obtained at the MPIC, Mainz (a) (pellets 1–6), and the CIGS (b) (pellet 7). The $^{87}Sr/^{86}Sr$ as well as the $^{84}Sr/^{86}Sr$ ratio of the individual measurements (black squares) is shown as well as the mean ratio (horizontal black line) and the respective 2*s* uncertainties (dashed lines).

analyses. Therefore, the analysis by LA-MC-ICP-MS is necessary to assess homogeneity at a scale of 10 s of µm. Individual measurements from the LA-MC-ICP-MS measurements at MPIC yielded results for the $^{87}Sr/^{86}Sr$ isotope ratios with small deviations in comparison with the mean solution ratio. Cross-checking with deviations in the $^{84}Sr/^{86}Sr$ ratio, as suggested by Müller and Anczkiewicz (2016), did not show an obvious correlation between a bias in $^{87}Sr/^{86}Sr$ and an elevated or reduced $^{84}Sr/^{86}Sr$ ratio, although the $^{84}Sr/^{86}Sr$ ratios of the LA-MC-ICP-MS analyses performed at MPIC are

lower than expected from the naturally invariant ratio. The trend in $^{84}Sr/^{86}Sr$ during both LA-MC-ICP-MS measurements (Figure 6) shows furthermore no relation to the formation of Ca argides/dimers, since monitoring of *m/z* 83 and 82 did not show a significant increase between the gas-blank period and during the ablation. In addition, the measurements were randomly distributed on different nanopowder pellets (pellets 1–6 for MPIC and pellet 7 for CIGS). Due to the solely use of 10^{11} Ω resistors, a more precise monitoring of the small signals observed at *m/z* 83 and *m/z* 82 was not possible to potentially detect small changes in Ca argide/dimer formation rate. However, we cannot entirely exclude further interference affecting the $^{84}Sr/^{86}Sr$ ratio. In general, the trend in $^{84}Sr/^{86}Sr$ does not imply that the $^{87}Sr/^{86}Sr$ results are inaccurate. Several studies showed that highly precise and accurate $^{87}Sr/^{86}Sr$ results can be paired with poor quality $^{84}Sr/^{86}Sr$ ratios (e.g., Horstwood *et al.* 2008, Copeland *et al.* 2010, Weber *et al.* 2018a). In these studies, the $^{84}Sr/^{86}Sr$ deviates even further from the accepted value than for our measurements. Both LA-MC-ICP-MS set-ups, however, yielded individual and mean $^{87}Sr/^{86}Sr$ ratios in agreement with the solution data ($^{87}Sr/^{86}Sr$ = 0.70756 ± 0.00003, 2*s*). In addition, the laser ablation trace element analyses were performed with even smaller test portion masses than the Sr isotope measurements. No significant deviation within one pellet was observed with this technique, further indicating that the NanoSr can be considered homogeneous for microanalytical *in situ* Sr isotope determinations on a scale of 10 s of µm. This implies that the flame spray technique is suitable to produce a custom-made microanalytical carbonate RM, which fulfils the requirements for microanalytical Sr isotope analysis.

Availability of NanoSr

In total, 15 g of the synthetic carbonate nanopowder NanoSr was produced. A single pressed pellet equals about 100 mg of carbonate nanopowder. Due to the intended use as widely available low-Sr carbonate reference material for the *in situ* measurement of Sr isotopes, aliquots of NanoSr are available on request from the corresponding author.

Conclusions

This study characterised a custom-made reference material with a specified mass fraction of Sr and a carbonate matrix. Due to the lack of a suitable low-Sr microanalytical carbonate reference material for *in situ* LA-MC-ICP-MS analysis of Sr isotopes, a synthetic carbonate nanomaterial with a relatively low-Sr mass fraction was produced using the flame spray method. The material can be easily pressed to stable nanopowder pellets and yielded clean ablation tracks. The trace element mass fraction was determined after digestion and using laser ablation ICP-MS and yielded a mass fraction of Sr of approximately 500 µg g^{-1}. Potentially interfering elements, such as Rb and REEs, did not affect Sr isotope analysis due to their low mass fraction. Determination of the Sr isotope ratios using LA-MC-ICP-MS in two laboratories with three different and independent solution-based techniques yielded results in agreement within uncertainty and a mean $^{87}Sr/^{86}Sr$ ratio of 0.70756 ± 0.00003 (2*s*). Therefore, the NanoSr can be used as a matrix-matched reference material for carbonate samples to monitor the accuracy and precision of microanalytical analyses of Sr isotopes. Furthermore, this proof-of-concept study confirms the possibility for researchers to produce their own microanalytical custom-made reference materials using the flame spray technique, not only for glass matrices but also for carbonates.

Acknowledgements

M. Weber, K.P. Jochum and D. Scholz are thankful to the Max Planck Graduate Centre and the German Research Foundation (DFG SCHO 1274/9-1 and DFG SCHO 1274/11-1). We are indebted to Anna Cipriani for the use of geochemical facilities at University of Modena and Reggio Emilia, as well as Steve Galer for the access to the TIMS instrument at MPIC. We also thank B. Stoll, U. Weis and M. Großkopf for assistance in the laboratory and S. Buhre and N. Groschopf for providing the EPMA data. We thank T. Häger for access to the hydraulic press. The authors thank the editor and two anonymous referees for their thorough reviews and constructive comments that helped to improve the article.

Conflicts of interest

There are no conflicts of interest to declare.

Data availability statement

The data that support the findings of this study are available in the supplementary material and from the corresponding author upon request.

References

Armstrong J.T. (1995)
Citzaf – A package of correction programs for the quantitative electron microbeam X-ray-analysis of thick polished materials, thin-films, and particles. **Microbeam Analysis**, **4**, 177–200.

references

Athanassiou E.K., Grass R.N. and Stark W.J. (2010)
Chemical aerosol engineering as a novel tool for material science: From oxides to salt and metal nanoparticles. Aerosol Science and Technology, 44, 161–172.

Banner J.L., Musgrove M.L., Asmerom Y., Edwards R.L. and Hoff J.A. (1996)
High-resolution temporal record of Holocene ground-water chemistry: Tracing links between climate and hydrology. Geology, 24, 1049–1053.

Bao Z., Chen L., Zong C., Yuan H., Chen K. and Dai M. (2017)
Development of pressed sulfide powder tablets for *in situ* sulfur and lead isotope measurement using LA-MC-ICP-MS. International Journal of Mass Spectrometry, 421, 255–262.

Berglund M. and Wieser M.E. (2011)
Isotopic compositions of the elements 2009 (IUPAC Technical Report). Pure and Applied Chemistry, 83, 397–410.

Bolea-Fernandez E., Van Malderen S.J.M., Balcaen L., Resano M. and Vanhaecke F. (2016)
Laser ablation-tandem ICP-mass spectrometry (LA-ICP- MS/MS) for direct Sr isotopic analysis of solid samples with high Rb/Sr ratios. Journal of Analytical Atomic Spectrometry, 31, 464–472.

Copeland S.R., Sponheimer M., Lee-Thorp J.A., le Roux P.J., de Ruiter D.J. and Richards M.P. (2010)
Strontium isotope ratios in fossil teeth from South Africa: Assessing laser ablation MC-ICP-MS analysis and the extent of diagenesis. Journal of Archaeological Science, 37, 1437–1446.

Durante C., Baschieri C., Bertacchini L., Bertelli D., Cocchi M., Marchetti A., Manzini D., Papotti G. and Sighinolfi S. (2015)
An analytical approach to Sr isotope ratio determination in Lambrusco wines for geographical traceability purposes. Food Chemistry, 173, 557–563.

Evans D. and Müller W. (2018)
Automated extraction of a five-year LA-ICP-MS trace element data set of ten common glass and carbonate reference materials: Long-term data quality, optimisation and laser cell homogeneity. Geostandards and Geoanalytical Research, 42, 159–188.

Fietzke J. and Eisenhauer A. (2006)
Determination of temperature-dependent stable strontium isotope ($^{88}Sr/^{86}Sr$) fractionation via bracketing standard MC-ICP-MS. Geochemistry, Geophysics, Geosystems, 7, Q08009.

Fietzke J., Liebetrau V., Günther D., Gurs K., Hametner K., Zumholz K., Hansteen T.H. and Eisenhauer A. (2008)
An alternative data acquisition and evaluation strategy for improved isotope ratio precision using LA-MC-ICP-MS applied to stable and radiogenic strontium isotopes in carbonates. Journal of Analytical Atomic Spectrometry, 23, 955–961.

Garbe-Schönberg D. and Müller S. (2014)
Nano-particulate pressed powder tablets for LA-ICP-MS. Journal of Analytical Atomic Spectrometry, 29, 990–1000.

Goede A., McCulloch M., McDermott F. and Hawkesworth C. (1998)
Aeolian contribution to strontium and strontium isotope variations in a Tasmanian speleothem. Chemical Geology, 149, 37–50.

Hori M., Ishikawa T., Nagaishi K., Lin K., Wang B.-S., You C.-F., Shen C.-C. and Kano A. (2013)
Prior calcite precipitation and source mixing process influence Sr/Ca, Ba/Ca and $^{87}Sr/^{86}Sr$ of a stalagmite developed in southwestern Japan during 18.0–4.5 ka. Chemical Geology, 347, 190–198.

Horstwood M.S.A., Evans J.A. and Montgomery J. (2008)
Determination of Sr isotopes in calcium phosphates using laser ablation inductively coupled plasma-mass spectrometry and their application to archaeological tooth enamel. Geochimica et Cosmochimica Acta, 72, 5659–5674.

Ingle C.P., Sharp B.L., Horstwood M.S.A., Parrish R.R. and Lewis D.J. (2003)
Instrument response functions, mass bias and matrix effects in isotope ratio measurements and semi-quantitative analysis by single and multi-collector ICP-MS. Journal of Analytical Atomic Spectrometry, 18, 219–229.

Irrgeher J., Galler P. and Prohaska T. (2016)
$^{87}Sr/^{86}Sr$ isotope ratio measurements by laser ablation multicollector inductively coupled plasma-mass spectrometry: Reconsidering matrix interferences in bioapatites and biogenic carbonates. Spectrochimica Acta Part B, 125, 31–42.

Jochum K.P. and Enzweiler J. (2014)
Reference materials in geochemical and environmental research. In: Turekian K.K. (ed.), Treatise on geochemistry (2nd edition). Elsevier (Oxford), 43–70.

Jochum K.P., Nohl L., Herwig K., Lammel E., Stoll B. and Hofmann A.W. (2005)
GeoReM: A new geochemical database for reference materials and isotopic standards. Geostandards and Geoanalytical Research, 29, 333–338.

Jochum K.P., Weis U., Stoll B., Kuzmin D., Yang Q., Raczek I., Jacob D.E., Stracke A., Birbaum K. and Frick D.A. (2011a)
Determination of reference values for NIST SRM 610–617 glasses following ISO guidelines. Geostandards and Geoanalytical Research, 35, 397–429.

Jochum K.P., Wilson S.A., Abouchami W., Amini M., Chmeleff J., Eisenhauer A., Hegner E., Iaccheri L.M., Kieffer B., Krause J., McDonough W.F., Mertz-Kraus R., Raczek I., Rudnick R.L., Scholz D., Steinhoefel G., Stoll B., Stracke A., Tonarini S., Weis D., Weis U. and Woodhead J.D. (2011b)
GSD-1G and MPI-DING reference glasses for *in situ* and bulk isotopic determination. Geostandards and Geoanalytical Research, 35, 193–226.

references

Jochum K.P., Scholz D., Stoll B., Weis U., Wilson S.A., Yang Q.C., Schwalb A., Borner N., Jacob D.E. and Andreae M.O. (2012)
Accurate trace element analysis of speleothems and biogenic calcium carbonates by LA-ICP-MS. Chemical Geology, 318, 31–44.

Jochum K.P., Garbe-Schönberg D., Veter M., Stoll B., Weis U., Weber M., Lugli F., Jentzen A., Schiebel R. and Wassenburg J.A. (2019)
Nano-powdered calcium carbonate reference materials: Significant progress for microanalysis? Geostandards and Geoanalytical Research. https://doi.org/10.1111/ggr.12292

Kane J.S., Potts P.J., Wiedenbeck M., Carignan J. and Wilson S. (2003)
International Association of Geoanalysts' protocol for the certification of geological and environmental reference materials. Geostandards Newsletter: The Journal of Geostandards and Geoanalysis, 27, 227–244.

Kelly S., Heaton K. and Hoogewerff J. (2005)
Tracing the geographical origin of food: The application of multi-element and multi-isotope analysis. Trends in Food Science and Technology, 16, 555–567.

Kimura J.I., Takahashi T. and Chang Q. (2013)
A new analytical bias correction for *in situ* Sr isotope analysis of plagioclase crystals using laser-ablation multiple-collector inductively coupled plasma-mass spectrometry. Journal of Analytical Atomic Spectrometry, 28, 945–957.

Krabbenhöft A., Fietzke J., Eisenhauer A., Liebetrau V., Böhm F. and Vollstaedt H. (2009)
Determination of radiogenic and stable strontium isotope ratios ($^{87}Sr/^{86}Sr$; $\delta^{88}/^{86}Sr$) by thermal ionization mass spectrometry applying an $^{87}Sr/^{84}Sr$ double spike. Journal of Analytical Atomic Spectrometry, 24, 1267–1271.

Lin J., Liu Y., Chen H., Zhou L., Hu Z. and Gao S. (2015)
Review of high-precision Sr isotope analyses of low-Sr geological samples. Journal of Earth Science, 26, 763–774.

Lugli F., Cipriani A., Peretto C., Mazzucchelli M. and Brunelli D. (2017)
In situ high spatial resolution $^{87}Sr/^{86}Sr$ ratio determination of two Middle Pleistocene (*ca.* 580 ka) *Stephanorhinus hundsheimensis* teeth by LA-MC-ICP-MS. International Journal of Mass Spectrometry, 412, 38–48.

Lugli F., Cipriani A., Tavaglione V., Traversari M. and Benazzi S. (2018)
Transhumance pastoralism of Roccapelago (Modena, Italy) early-modern individuals: Inferences from Sr isotopes of hair strands. American Journal of Physical Anthropology, 167, 470–483.

McArthur J.M., Howarth R.J. and Bailey T.R. (2001)
Strontium isotope stratigraphy: LOWESS Version 3: Best fit to the marine Sr-isotope curve for 0–509 Ma and accompanying look-up table for deriving numerical age. Journal of Geology, 109, 155–170.

McArthur J.M., Howarth R.J. and Shields G.A. (2012)
Strontium isotope stratigraphy. The geologic time scale, 1, 127–144.

Mischel S.A., Mertz-Kraus R., Jochum K.P. and Scholz D. (2017)
TERMITE: An R script for fast reduction of laser ablation inductively coupled plasma-mass spectrometry data and its application to trace element measurements. Rapid Communications in Mass Spectrometry, 31, 1079–1087.

Müller W. and Anczkiewicz R. (2016)
Accuracy of laser-ablation (LA)-MC-ICP-MS Sr isotope analysis of (bio) apatite – A problem reassessed. Journal of Analytical Atomic Spectrometry, 31, 259–269.

Ohno T. and Hirata T. (2007)
Simultaneous determination of mass-dependent isotopic fractionation and radiogenic isotope variation of strontium in geochemical samples by multiple collector-ICP-mass spectrometry. Analytical Science, 23, 1275–1280.

Oster J.L., Montañez I.P., Mertz-Kraus R., Sharp W.D., Stock G.M., Spero H.J., Tinsley J. and Zachos J.C. (2014)
Millennial-scale variations in western Sierra Nevada precipitation during the last glacial cycle MIS 4/3 transition. Quaternary Research, 82, 236–248.

Poitrasson F., Mao X., Mao S.S., Freydier R. and Russo R.E. (2003)
Comparison of ultraviolet femtosecond and nanosecond laser ablation inductively coupled plasma-mass spectrometry analysis in glass, monazite, and zircon. Analytical Chemistry, 75, 6184–90.

Sforna M.-C. and Lugli F. (2017)
MapIT!: A simple and user-friendly MATLAB script to elaborate elemental distribution images from LA-ICP-MS data. Journal of Analytical Atomic Spectrometry, 32, 1035–1043.

Steiger R.H. and Jäger E. (1977)
Subcommission on geochronology: Convention on the use of decay constants in geo- and cosmochronology. Earth and Planetary Science Letters, 36, 359–362.

Tabersky D., Luechinger N.A., Rossier M., Reusser E., Hametner K., Aeschlimann B., Frick D.A., Halim S.C., Thompson J. and Danyushevsky L. (2014)
Development and characterization of custom-engineered and compacted nanoparticles as calibration materials for quantification using LA-ICP-MS. Journal of Analytical Atomic Spectrometry, 29, 955–962.

Vanhaecke F., Resano M., Koch J., McIntosh K. and Günther D. (2010)
Femtosecond laser ablation-ICP-mass spectrometry analysis of a heavy metallic matrix: Determination of platinum-group metals and gold in lead fire-assay buttons as a case study. Journal of Analytical Atomic Spectrometry, 25, 1259.

Vroon P.Z., van der Wagt B., Koornneef J.M. and Davies G.R. (2008)
Problems in obtaining precise and accurate Sr isotope analysis from geological materials using laser ablation MC-ICP-MS. Analytical and Bioanalytical Chemistry, 390, 465–76.

references

Weber M., Wassenburg J.A., Jochum K.P., Breitenbach S.F.M., Oster J. and Scholz D. (2017)
Sr-isotope analysis of speleothems by LA-MC-ICP-MS: High temporal resolution and fast data acquisition. **Chemical Geology, 468**, 63–74.

Weber M., Lugli F., Jochum K.P., Cipriani A. and Scholz D. (2018a)
Calcium carbonate and phosphate reference materials for monitoring bulk and microanalytical determination of Sr isotopes. **Geostandards and Geoanalytical Research, 42**, 77–89.

Weber M., Scholz D., Schröder-Ritzrau A., Deininger M., Spötl C., Lugli F., Mertz-Kraus R., Jochum K.P., Fohlmeister J. and Stumpf C.F. (2018b)
Evidence of warm and humid interstadials in central Europe during early MIS 3 revealed by a multi-proxy speleothem record. **Quaternary Science Reviews, 200**, 276–286.

Willmes M., Kinsley L., Moncel M.H., Armstrong R.A., Aubert M., Eggins S. and Grün R. (2016)
Improvement of laser ablation *in situ* micro-analysis to identify diagenetic alteration and measure strontium isotope ratios in fossil human teeth. **Journal of Archaeological Science, 70**, 102–116.

Woodhead J., Swearer S., Hergt J. and Maas R. (2005)
In situ Sr-isotope analysis of carbonates by LA-MC-ICP-MS: interference corrections, high spatial resolution and an example from otolith studies. **Journal of Analytical Atomic Spectrometry, 20**, 22.

Wortham B.E., Wong C.I., Silva L.C.R., McGee D., Montañez I.P., Rasbury E.T., Cooper K.M., Sharp W.D., Glessner J.J.G. and Santos R.V. (2017)
Assessing response of local moisture conditions in central Brazil to variability in regional monsoon intensity using speleothem $^{87}Sr/^{86}Sr$ values. **Earth and Planetary Science Letters, 463**, 310–322.

Wu S., Karius V., Schmidt B.C., Simon K. and Wörner G. (2018)
Comparison of ultrafine powder pellet and flux-free fusion glass for bulk analysis of granitoids by laser ablation-inductively coupled plasma-mass spectrometry. **Geostandards and Geoanalytical Research, 42**, 575–591.

Yang Z.P., Fryer B.J., Longerich H.P., Gagnon J.E. and Samson I.M. (2011)
785 nm femtosecond laser ablation for improved precision and reduction of interferences in Sr isotope analyses using MC-ICP-MS. **Journal of Analytical Atomic Spectrometry, 26**, 341–351.

Zhou H., Feng Y.-X., Zhao J.-X., Shen C.-C., You C.-F. and Lin Y. (2009)
Deglacial variations of Sr and $^{87}Sr/^{86}Sr$ ratio recorded by a stalagmite from Central China and their association with past climate and environment. **Chemical Geology, 268**, 233–247.

Supporting information

The following supporting information may be found in the online version of this article:

Figure S1. Ablation pits on NanoSr from spot analyses with the NWR193 laser ablation system and from line scan analyses with the UP213 nm laser ablation system.

Table S1. QCM results for LA-ICP-MS analyses performed at MPIC, Mainz.

Table S2. QCM results for LA-ICP-MS analyses performed at Institute of Geosciences, Mainz.

Tables S3–S14. LA-ICP-MS, ICP-MS, MC-ICP-MS, LA-MC-ICP-MS, TIMS and EPMA results performed at the laboratories involved in this study.

This material is available from: http://onlinelibrary.wiley.com/doi/10.1111/ggr.12296/abstract (This link will take you to the article abstract).